Bioorganic & Medicinal Chemistry 20 (2012) 6073–6079

Contents lists available at SciVerse ScienceDirect

Bioorganic & Medicinal Chemistry

journal homepage: www.elsevier.com/locate/bmc

Selection, synthesis, and anti-inflammatory evaluation of the arylidene malonate derivatives as TLR4 signaling inhibitors

Shuting Zhang, Kui Cheng, Xiaohui Wang, Hang Yin *

Department of Chemistry and Biochemistry and BioFrontiers Institute, 596 University of Colorado at Boulder, Boulder, CO 80309-0596, USA

ARTICLE INFO

Article history:
Received 2 June 2012
Revised 11 August 2012
Accepted 19 August 2012
Available online 25 August 2012

Keywords:
Toll-like receptor 4
NF-κB
Arylidene malonate
Anti-inflammation

ABSTRACT

Inhibition of TLR4 signaling is an important therapeutic strategy for intervention in the etiology of several pro-inflammatory diseases. There has been intensive research in recent years aiming to explore this strategy, and identify small molecule inhibitors of the TLR4 pathway. However, the recent failure of a number of advanced drug candidates targeting TLR4 signaling (*e.g.*, TAK242 and Eritoran) prompted us to continue the search for novel chemical scaffolds to inhibit this critical inflammatory response pathway. Here we report the identification of a group of new TLR4 signaling inhibitors through a cell-based screening. A series of arylidene malonate analogs were synthesized and assayed in murine macrophages for their inhibitory activity against LPS-induced nitric oxide (NO) production. The lead compound **1** (NCI126224) was found to suppress LPS-induced production of nuclear factor-kappaB (NF-κB), tumor necrosis factor (TNF-α), interleukin-1β (IL-1β), and nitric oxide (NO) in the nanomolar-low micromolar range. Taken together, this study demonstrates that **1** is a promising potential therapeutic candidate for various inflammatory diseases.

1. Introduction

The first line of defense in host protection against invading microbial pathogens is the innate immune system, where the Toll-like receptors (TLRs) play a critical role.[1] TLRs function to detect and respond to a series of structurally conserved molecules known as pathogen-associated molecular patterns (PAMPs). Response to PAMPs by TLRs leads to the up-regulation of pro-inflammatory cytokines and mediators, initiating the innate immune response. The first identified and most well studied TLR is TLR4, which recognizes lipopolysaccharide (LPS) or endotoxin, a major component of the outer membrane of Gram-negative bacteria.[2–4] LPS-induced TLR4 signal transduction requires the association of the accessory protein myeloid differentiation factor 2 (MD-2) to TLR4. Binding of LPS to the large hydrophobic pocket on the MD-2 surface induces the homodimerization of two copies of the MD-2–TLR4–LPS complex.[5]

This homodimerization diverges to result in the activation of either myeloid differentiation primary-response gene 88 (MyD88)-dependent, or Toll/interleukin-1 receptor domain-containing adaptor inducing IFN-β (TRIF)-dependent signaling.[6] MyD88-dependent signaling induces NF-κB activation as an inflammatory response. Under normal circumstances, NF-κB remains sequestered in the cytoplasm as an inactive complex by a family of inhibitory proteins known as IκBs.[7] Upon binding to MD-2 in the presence of LPS, TLR4 initiates a series of phosphorylation events resulting in the phosphorylation of the cytoplasmic IκBs. These phosphorylated IκBs then undergo ubiquitylation and subsequent degradation by the proteasome, resulting in the translocation of NF-κB into the nucleus.[8,9] Nuclear NF-κB promotes transcription of various proinflammatory cytokines including inducible nitric oxide synthase (iNOS), cyclooxygenase-2 (COX-2), tumor necrosis factor (TNF)-α, interleukin-1β (IL-1β), and IL-6.[10,11] In contrast, TRIF-dependent signaling activates interferon regulatory factor 3 (IRF3), which induces type I interferon (IFN) expression.[12,13]

Although LPS-induced proinflammatory cytokine production initiates the host defense against injury and infection,[14,15] the dysregulation of TLR4 signaling contributes to an array of acute and chronic human diseases such as septic shock, inflammatory arthritis, atherosclerosis, and cancer.[16–19] Its involvement in human disease makes the TLR4 signaling pathway an important therapeutic target.[20] In fact, several TLR4 signaling inhibitors have already been investigated as potential anti-sepsis drugs. The most advanced of these, TAK242 and Eritoran,[21,22] were successful in pre-clinical trials but both failed in Phase III clinical trials due to lack of efficacy.[23,24] Therefore, the identification of new TLR4 signaling inhibitors which serve as novel therapeutics is still an urgent need.

In the present study, we identified a group of novel TLR4 signaling inhibitors, developed from our initial lead 2-(2-nitrobenzylidene) malonate (**1**), and investigated their structure-activity relationship. Further, we examined the inhibitory effects of **1** on

* Corresponding author. Tel.: +1 303 492 6786.
E-mail address: Hubert.Yin@Colorado.edu (H. Yin).

0968-0896/$ - see front matter © 2012 Elsevier Ltd. All rights reserved.
http://dx.doi.org/10.1016/j.bmc.2012.08.022

downstream NF-κB activation to elucidate the mechanism of its inhibitory effects.

2. Results and discussion

2.1. Screening for TLR4 signaling inhibitors

We interrogated the 1363-member Diversity Set II library from the National Cancer Institute (NCI) for inhibition of LPS-induced NO production using murine macrophage RAW 264.7 cells as previously reported.[25] This library consists of small molecules that were selected from the larger 140,000-compound NCI library on the basis of availability, purity, and other diversity criteria. After the preliminary screening, a total of six compounds were identified that showed >80% inhibitory activity at a concentration of 1.0 μM. To ensure that the observed inhibition was not due to cell proliferation inhibition, we used the previously established WST-1 toxicity assay to determine the cytotoxicity of the six selected hits.[26] Only one compound, NCI126224 (**1**, Scheme 1) based on an arylidene malonate scaffold did not show significant toxicity up to 10.0 μM, prompting us to focus on this scaffold for further investigation.

2.2. Structure-activity relationship studies of the arylidene malonate derivatives

Next, we performed structure-activity relationship (SAR) studies of the selected hit compound, **1**, to identify the key structural features essential for inhibitory activity. The representative synthetic route for **1**–**21** is shown in Scheme 1. Commercially available dimethyl malonate underwent a piperidine-catalyzed Knoevenagel condensation with various aldehydes, affording **1**–**16** and **21** in good yields. Then, the resultant Compounds **1**–**3** and **10** were converted to the corresponding diacids, **17**–**20**, by hydrolysis with potassium hydroxide. Dimethyl malonate was treated with sodium hydride, then 2-nitrobenzyl chloride to give the fully saturated analog **22** (Scheme 2). Compound **23** was obtained from the condensation of 2-nitrobenzaldehyde and malonic acid followed by methyl-esterification (Scheme 3).

As shown in Table 1 and 12 compounds exhibited submicromolar IC_{50} values for inhibition of LPS-induced NO production in RAW 264.7 cells. As a comparison, their inhibitory activities were significantly higher than the widely used anti-inflammatory agent, curcumin (IC_{50} = 6 μM).[27] To study the influence of the α,β-double bond, reduced analog (**22**) of **1** was evaluated. The reduction of the

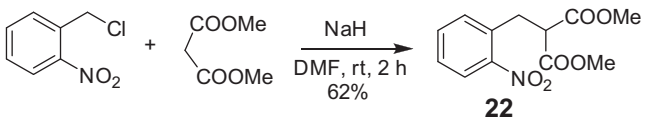

Scheme 2. Synthesis of compound **22**.

α,β-double bond resulted in a complete loss of inhibitory activity (IC_{50} >100 μM), so compound **22** was used as the negative control in the subsequent biological evaluations. This demonstrates that the presence of Michael acceptor maybe essential for its TLR4 signaling inhibitory activity. This property is consistent with TAK242, a known TLR inhibitor that covalently binds to Cys747 in TLR4 via a Michael reaction.[28]

Covalent inhibitors are rarely considered when initiating a target-directed drug discovery project due to safety concerns. Nonetheless, a relatively potent inhibitor may render an activity window that allows useful applications of specifically regulating the TLR4-mediated inflammation response. Furthermore, the recent revived interests of covalent drugs also suggest that such molecules could still serve as promising drug candidates in principle.[29] Figure 1A showed a representative dose-response analysis of **1** to assess the IC_{50} values for inhibition of LPS-induced NO production in the RAW 264.7 cells in comparison with **22**. The results showed that **1** potently blocked LPS-induced NO production with an IC_{50} of 0.31 ± 0.03 μM. By contrast, compound **22** showed negligible inhibition at the tested concentrations.

Replacement of the phenyl ring with a cyclohexyl ring (**21**) resulted in reduced activity. Additionally, the monoester (**23**) was less potent than the corresponding diester (**1**). The effect of the arylidene malonate pharmacophore on TLR4 signaling was also investigated with regard to the electronic properties of phenyl substituent. As shown in Table 1, the *ortho*-substituted arylidene malonates (**1**, **3**, **5**) were remarkably more potent than their *meta*-substituted counterparts (**14**, **15**, **16**). The corresponding *para*-substituted analogs (**6**, **7**, **10**) were slightly less potent than the *ortho*-substituted analogs. Further SAR studies revealed that the presence of a strong electron-withdrawing group on the 2-position of the benzene ring remarkably increased the inhibitory activity. This suggests that the electron deficiency aromatic ring is critical for compound efficacy. When the nitro group at the 2-position was replaced with fluorine (**3**), no significant inhibitory potency change was observed. By contrast, the introduction of a methoxy group to the 2-position (**5**) led to a decreased inhibitory activity.

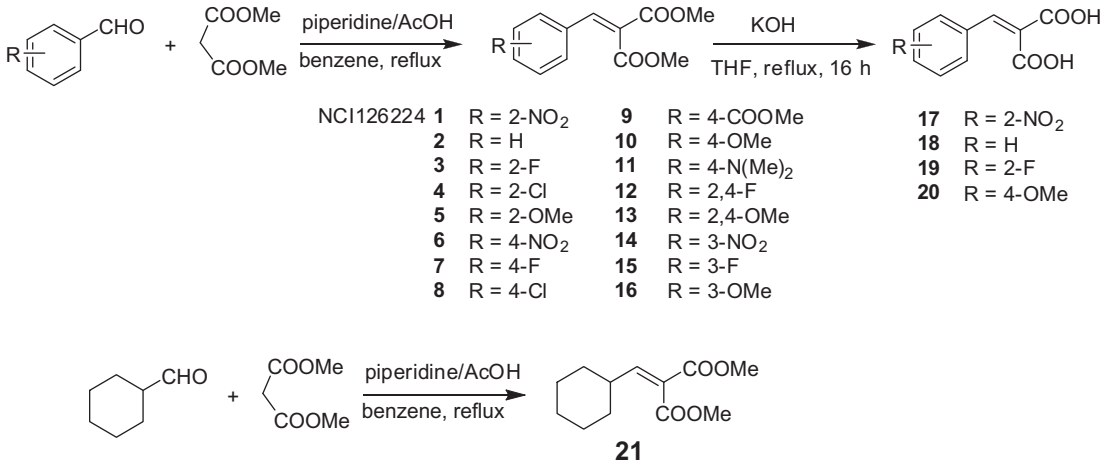

Scheme 1. Generic synthesis route of compounds **1**–**21**.

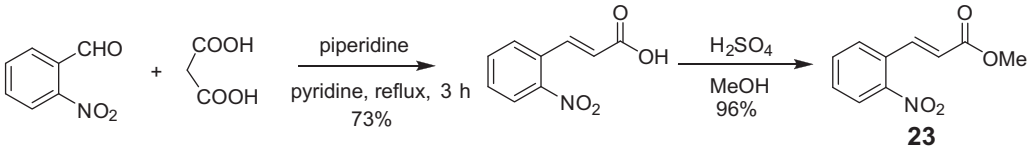

Scheme 3. Synthesis of compound **23.**

Table 1
Inhibitory effects of the arylidene malontate derivatives on LPS-induced NO production in RAW 264.7 macrophage cells

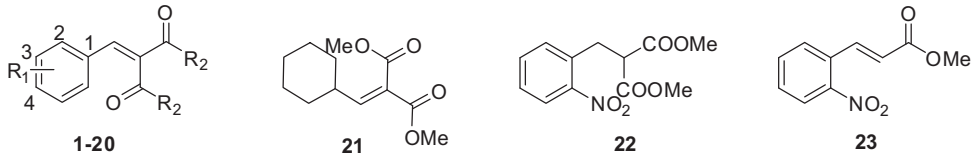

	R1	R2	IC_{50} (μM)
1 (NCI126224)	2-NO_2	OMe	0.31 ± 0.03
2	H	OMe	0.82 ± 0.08
3	2-F	OMe	0.33 ± 0.14
4	2-Cl	OMe	0.82 ± 0.15
5	2-OMe	OMe	0.74 ± 0.26
6	4-NO_2	OMe	0.82 ± 0.04
7	4-F	OMe	0.71 ± 0.14
8	4-Cl	OMe	1.54 ± 0.22
9	4-COOMe	OMe	1.33 ± 0.05
10	4-OMe	OMe	1.24 ± 0.12
11	4-$N(Me)_2$	OMe	3.11 ± 0.26
12	2,4-F	OMe	0.42 ± 0.08
13	2,4-OMe	OMe	0.82 ± 0.27
14	3-NO_2	OMe	2.13 ± 0.26
15	3-F	OMe	2.53 ± 0.31
16	3-OMe	OMe	3.72 ± 0.36
17	2-NO_2	OH	0.52 ± 0.12
18	2-F	OH	0.41 ± 0.16
19	H	OH	0.93 ± 0.07
20	4-OMe	OH	1.44 ± 0.18
21			78.2 ± 1.6
22			>100
23			4.53 ± 0.36

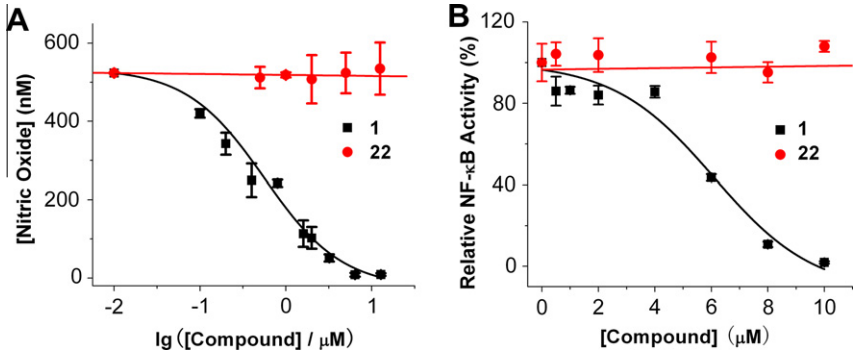

Figure 1. (A) Representative dose-dependent inhibitory response of the arylidene malonate analogs on LPS-induced NO production in RAW 264.7 macrophage cells. (B) Effects of **1** and the negative control, **22**, on LPS-induced activation of NF-κB using a NF-κB dual luciferase reporter assay in BV-2 microglial cells.

With the absence of any substituent on the benzene ring (**2**) the activity decreased by greater than 2-fold. It was also determined that the malonic acid derivatives (**17**–**20**) were less active than the corresponding ester analogs (R_2 = methoxy group). Nevertheless, these di-acid derivatives were still effective TLR4 signaling inhibitors with IC_{50} values in the low micromolar range. Taken together, these results suggest that arylidene malontate derivatives present a consistent SAR and small modifications of its core significantly affect its inhibitory potency, implying a near optimal recognition of its potential target.

2.3. Effect of 1 on downstream NF-κB activation

Induction of the TLR4 signaling pathway stimulates the activation of NF-κB through both the MyD88- and TRIF-dependent pathways. NF-κB activation upregulates iNOS, resulting in elevated production of NO. To determine whether the inhibition of NO production by **1** is due to the suppression of NF-κB activation, an NF-κB luciferase reporter gene assay was performed. NF-κB dual-luciferase reporter in BV-2 cells, a widely used microglial cell line expressing various TLR receptors,[30] were incubated with LPS

(200 ng/mL) in the absence or presence of **1** or the negative control, compound **22**, for 24 h. NF-κB reporter activity was increased by 45-fold after LPS treatment and this increase was diminished in cells treated with **1** in a dose-dependent manner (Fig. 1B). The IC_{50} value obtained for **1** was 5.92 ± 0.14 μM. By contrast, the inactive compound, **22**, did not alter the LPS-induced NF-κB activation at concentrations up to 10 μM. This result suggests that **1** inhibits the TLR4 signaling pathway upstream of NF-κB activation, which is in a good agreement with its inhibitory activity of the NO production.

2.4. Effect of 1 on downstream cytokines production

LPS-induced TLR4 activation results in an increased production of the proinflammatory cytokines, IL-1β and TNF-α. To further understand the mechanism of TLR4 signaling inhibition by **1**, we examined its effect on LPS-induced production of two cytokines, IL-1β and TNF-α, in macrophages using a previously developed ELISA assay.[31] LPS treatment resulted in the production of significant elevation of the IL-1β and TNF-α levels compared to vehicle treated cells, reaching a maximum of approximately 20-fold and 10-fold after 24 h, respectively. LPS-induced IL-1β production in macrophages was potently inhibited by **1** in a dose-dependent manner, with an IC_{50} value of 0.42 ± 0.15 μM (Fig. 2A). Similarly, LPS-induced TNF-α production was decreased in the presence of **1**, with a measured IC_{50} value of 1.54 ± 0.17 μM (Fig. 2B). By contrast, the inactive compound **22** did not affect the production of either IL-1β or TNF-α. Thus, **1** can efficiently block the LPS-induced production of several different cytokines in macrophages, which is in good agreement with our observations of its activities in NO and NF-κB inhibition.

2.5. Selectivity and specificity of 1

As previously discussed, a potential pitfall for **1** is its specificity due to its ability to serve as a Michael acceptor. In order to determine if **1** selectively inhibits the TLR4 signaling, the effects of **1** on other murine analogous TLRs were investigated using a previously reported method with RAW 264.7 macrophage cells that can be activated by different TLR-specific ligands.[32] At a concentration of 0.6 μM, **1** showed negligible inhibition to TLR1/TLR2, TLR3, or TLR7/8, suggesting that **1** is TLR4-specific (Fig. 3). Interestingly, it reduced the signal via the TLR2/TLR6 heterodimer for reasons yet to be identified (see further discussion *vide infra*).

2.6. Molecular docking of 1 to the TLR4-MD-2 interface

Based on the evidence that **1** inhibits the TLR4 signaling pathway but also affects the TLR2/TLR6 signaling pathway, we speculated that a potential binding mode for **1** is that it might disrupt the TLR4 signaling by interacting with MD-2, complex as TLR4 and TLR2 are the only TLRs that have been reported to require an accessory protein, MD-2, to initiate their signaling.[33] It would be conceivable that an inhibitor that targets the MD-2 interface with TLR4 or TLR2/6 might selectively block TLR2 and TLR4 over other TLRs. To further explore this hypothesis, a computational docking search was carried out to determine if there is a desired binding mode of **1** to the TLR4/MD-2 protein interface (TLR2/MD-2 structure remains unsolved). As shown in Figure 4, in the most energetically favorable predicted binding mode, **1** was found to fit into the LPS-binding site of TLR4-MD-2 complex exhibiting close contacts with Gln436 of TLR4, as well as Lys122 and Ser120 in the Phe126 loop of MD-2. The entire structure of **1** was buried inside the LPS-binding pocket where the carbonyl group could form a hydrogen bond with the Gln436 residue on the TLR4 surface. Interestingly, the hydrophilic residues in the Phe126 loop of MD-2 and the Gln436 residue on TLR4 are known to be important for the interaction between LPS and TLR4-MD-2. These docking results implied a possible binding mode of **1** as a disruptor of the TLR4-MD-2 protein–protein interactions.

In summary, we have identified, synthesized and evaluated a series of arylidene malonate analogs as TLR4 signaling inhibitors. SAR studies have determined the important structural requirements

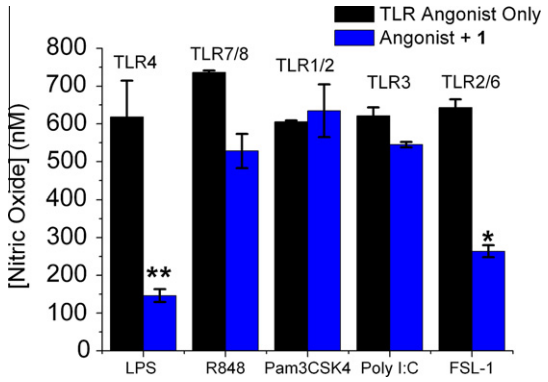

Figure 3. Inhibitory effects of **1** on the NO production induced by various TLR-specific ligands in RAW 264.7 cells. LPS (lipopolysaccharide), R848 {4-amino-2-(ethoxymethyl)-*R*,*R*-dimethyl-1*H*-imidazo[4,5-*c*]quinoline-1-ethanol}, Pam_3CSK_4 {*N*-palmitoyl-*S*-[2,3-bis(palmitoyloxy)-(2*R*,*S*)-propyl]-[*R*]-cysteinyl-[*S*]-seryl-[*S*]-lysyl-[*S*]-lysyl-[*S*]-lysyl-[*S*]-lysine·3HCl}, poly(I:C) (polyriboinosinic:polyribocytidylic acid), and FSL-1[(*S*,*R*)-(2,3-bispalmitoyloxypropyl)-Cys-Gly-Asp-Pro-Lys-His-Pro-Lys-Ser-Phe], were used to selectively activate TLR4, TLR7/8, TLR2/1, TLR3, and TLR2/6, respectively, in the presence or absence of 0.6 μM **1**. Data present the mean values (±SD) of three separate experiments, each performed in triplication (significance vs LPS alone treated group, $^{**}P < 0.01$; significance vs FSL-1 alone treated group, $^{*}P < 0.01$).

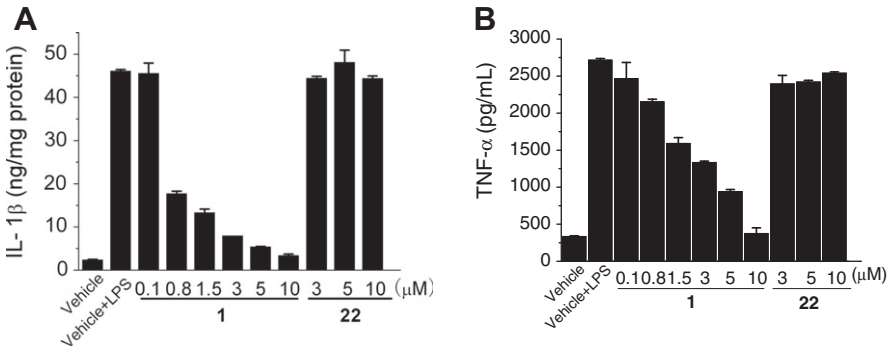

Figure 2. (A) Dose-dependence effects of **1** and **22** on LPS-induced IL-1β production in the RAW 264.7 cells. (B) Dose-dependence effects of **1** and **22** on the LPS-induced TNF-α production in the RAW 264.7 cells.

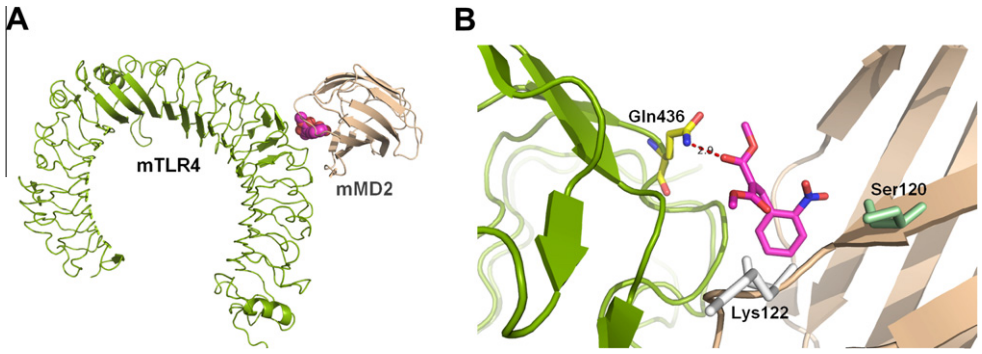

Figure 4. Molecular docking of **1** to the TLR4–MD-2 complex. (A) Docking simulation of **1** to the crystal structure of the human TLR4-MD-2 complex was performed using Glide 5.6. Molecular modeling of **1** in the LPS-binding site of the TLR4–MD-2 complex is represented as **1** by the magenta sphere, TLR4 is shown in green ribbon and MD-2 in light orange ribbon. (B) A close-up view of the predicted interaction between **1** and the LPS-binding site of the TLR4–MD-2 complex. TLR4 is shown in green and MD-2 in light orange.

for the high potency observed with the lead compound, **1**. Furthermore, **1** was found to inhibit LPS-mediated NF-κB activation and the cytokine production of IL-1β and TNF-α. A possible mechanism of **1** targeting the TLR4-MD-2 interface was proposed.

3. Materials and methods

3.1. Chemistry

Chemicals were purchased from Sigma Aldrich Chemical Co. TLC was performed on glass plates precoated by silica gel with visualization by UV-light. ^{1}H NMR and ^{13}C NMR spectra were recorded on a Bruker 300 or 400 MHz instrument and were referenced internally to the residual solvent peak. A compound library consisting of 1364 compounds was obtained from the National Cancer Institute Development Therapeutics Program repository (http://www.dtp.nci.nih.gov/index.html).

Compound **22** and **23** were prepared by following the literature procedures (Schemes 2 and 3).[34,35] The preparation of alkylidene and arylidene malonates (**1**–**16**, **21**) is through Knoevenagel Condensation of malonates and carbonyl compounds. The synthetic sequence is outlined in Scheme 1. A mixture of aldehyde (3.5 mmol), dimethyl malonate (3.5 mmol), acetic acid (10 μL) and piperdine (20 μL) in benzene (1.5 mL) was heated under reflux with azeotropic removal of water overnight. Benzene was removed by rotavapor, the residue was diluted with ethyl acetate (20 mL), washed with 10 percent hydrochloric acid, saturated sodium bicarbonate and brine. The organic layer was dried over anhydrous sodium sulfate, concentrated in vacuo and the residue was purified by silica chromatography to provide pure product.

As shown in Scheme 1, the diester (2 mmol) was dissolved in methanol (1.5 mL) and treated with a solution of KOH (0.23 g, 4 mmol) in water (1 mL), and the mixture was diluted with a minimum volume of THF to provide for its homogeneity. The reaction was heated under reflux for 16 h and concentrated in vacuo. This residue was dissolved in a minimum of water, and extracted with Et_2O. The aqueous layer was acidified with 17.5% hydrochloric acid to pH 3–4 and extracted with Et_2O. The ethereal extract was washed with water, dried over anhydrous sodium sulfate and evaporated. Products were purified by recrystallization or by precipitating them with hexane from the ethereal solution.

Dimethyl 2-(2-nitrobenzylidene)malonate **1**: yield: 75%. ^{1}H NMR (300 MHz, $CDCl_3$) δ 8.25–8.22 (m, 2H), 7.76–7.53 (m, 2H), 7.44–7.41 (m, 1H), 3.90 (s, 3H), 3.62 (s, 3H).

Dimethyl 2-benzylidenemalonate **2**: yield: 86%. ^{1}H NMR (300 MHz, $CDCl_3$) δ 8.09 (s, 1H), 7.48–7.29 (m, 4H), 7.28–7.23 (m, 1H), 3.89 (s, 3H), 3.77 (s, 3H).

Dimethyl 2-(2-fluorobenzylidene) malonate **3**: yield: 89%. ^{1}H NMR (300 MHz, $CDCl_3$) δ 7.96 (s, 1H), 7.45–7.37 (m, 2H), 7.19–7.09 (m, 2H), 3.88 (s, 3H), 3.84 (s, 3H).

Dimethyl 2-(2-chlorobenzylidene) malonate **4**: yield: 73%. ^{1}H NMR (300 MHz, $CDCl_3$) δ 8.09 (s, 1H), 7.47–7.34 (m, 3H), 7.33–7.27 (m, 1H), 3.89 (s, 3H), 3.77 (s, 3H).

Dimethyl 2-(2-methoxybenzylidene) malonate **5**: yield: 66%. ^{1}H NMR (300 MHz, $CDCl_3$) δ 8.13 (s, 1H), 7.42–7.33 (m, 2H), 6.97–6.90 (m, 2H), 3.87 (s, 3H), 3.86 (s, 3H), 3.80 (s, 3H).

Dimethyl 2-(4-nitrobenzylidene) malonate **6**: yield: 79%. ^{1}H NMR (300 MHz, $CDCl_3$) δ 8.29–8.24 (m, 2H), 7.82 (s, 1H), 7.63–7.58 (m, 2H), 3.90 (s, 3H), 3.86 (s, 3H).

Dimethyl 2-(4-fluorobenzylidene) malonate **7**: yield: 74%. ^{1}H NMR (300 MHz, $CDCl_3$) δ 7.74 (s, 1H), 7.50–7.38 (m, 2H), 7.09 (m, 2H), 3.86 (s, 3H), 3.86 (s, 3H).

Dimethyl 2-(4-chlorobenzylidene) malonate **8**: yield: 83%. ^{1}H NMR (300 MHz, $CDCl_3$) δ 7.73 (s, 1H), 7.37 (s, 4H), 3.86 (s, 3H), 3.86 (s, 3H).

Dimethyl 2-(4-(methoxycarbonyl)benzylidene) malonate **9**: yield:71%. ^{1}H NMR (300 MHz, $CDCl_3$) δ 8.04 (d, J = 8.3 Hz, 2H), 7.79 (s, 1H), 7.48 (d, J = 8.3 Hz, 2H), 3.92 (s, 3H), 3.86 (s, 3H), 3.83 (s, 3H).

Dimethyl 2-(4-methoxybenzylidene) malonate **10**: yield: 66%. ^{1}H NMR (300 MHz, $CDCl_3$) δ 7.72 (s, 1H), 7.39 (d, J = 6.8 Hz, 2H), 6.90 (d, J = 6.8 Hz, 2H), 3.87 (s, 3H), 3.84 (s, 6H).

Dimethyl 2-(4-(dimethylamino)benzylidene)malonate **11**: yield: 63%. ^{1}H NMR (300 MHz, $CDCl_3$) δ 7.69 (s, 1H), 7.35 (dd, J = 9.1, 0.4 Hz, 2H), 6.65 (d, J = 9.0 Hz, 2H), 3.90 (s, 3H), 3.83 (s, 3H), 3.05 (s, 6H).

Dimethyl 2-(2.4-difluorobenzylidene) malonate **12**: yield: 85%. ^{1}H NMR (300 MHz, $CDCl_3$) δ 7.86 (s, 1H), 7.52–7.33 (m, 1H), 6.96–6.78 (m, 2H), 3.86 (s, 3H), 3.83 (s, 3H). ^{13}C NMR (101 MHz, $CDCl_3$) δ166.43 (s), 164.28 (dd, J_{CF} = 253.0, 12.0 Hz), 164.09 (s), 161.39 (dd, J_{CF} = 256.2, 12.2 Hz), 134.44 (dd, J_{CF} = 4.6, 1.2 Hz), 130.48 (dd, J_{CF} = 10.1, 3.6 Hz), 127.13 (s), 117.57 (dd, J_{CF} = 12.5, 4.0 Hz), 112.05 (dd, J_{CF} = 21.7, 3.7 Hz), 104.54 (t, J_{CF} = 25.6 Hz), 52.78 (s), 52.68 (s). MS (ESI$^+$) m/z: 279.0 (M+Na), 257.1 (M+H$^+$).

Dimethyl 2-(2.4-dimethoxybenzylidene) malonate **13**: yield: 75%. ^{1}H NMR (300 MHz, $CDCl_3$) δ 8.09 (s, 1H), 7.32 (d, J = 8.5 Hz, 1H), 6.50–6.44 (m, 2H), 3.86 (s, 3H), 3.85 (s, 3H), 3.84 (s, 3H), 3.83 (s, 3H).

Dimethyl 2-(3-nitrobenzylidene) malonate **14**: yield: 69%. ^{1}H NMR (400 MHz, $CDCl_3$) δ 8.38–8.31 (m, 1H), 8.31–8.25 (m, 1H), 7.82 (s, 1H), 7.78–7.74 (m, 1H), 7.65–7.59 (m, 1H), 3.92 (s, 3H), 3.91 (s, 3H).

Dimethyl 2-(3-fluorobenzylidene) malonate **15**: yield: 73%. ^{1}H NMR (400 MHz, $CDCl_3$) δ 7.73 (s, 1H), 7.41–7.34 (m, 1H), 7.25–7.19 (m, 1H), 7.17–7.07 (m, 2H), 3.87 (s, 6H).

Dimethyl 2-(3-methoxybenzylidene) malonate **16**: yield: 85%. ^{1}H NMR (400 MHz, $CDCl_3$) δ 7.77 (s, 1H), 7.36–7.29 (m, 1H), 7.07–7.01 (m, 1H), 7.01–6.92 (m, 2H), 3.87 (s, 6H), 3.83 (s, 3H).

2-(2-nitrobenzylidene)malonic acid **17**: yield: 52%. ^{1}H NMR (400 MHz, DMSO) δ 8.24–8.15 (m, 1H), 7.93 (s, 1H), 7.84–7.79 (m, 1H), 7.72–7.67 (m, 1H), 7.54–7.51 (m, 1H).

2-benzylidene malonic acid **18**: yield: 55%. ^{1}H NMR (400 MHz, DMSO) δ 7.63–7.55 (m, 2H), 7.54 (s, 1H), 7.48–7.42 (m, 3H).

2-(2-fluorobenzylidene)malonic acid **19**: yield: 46%. ^{1}H NMR (400 MHz, DMSO) δ 7.62 (s, 1H), 7.61–7.56 (m, 1H), 7.54–7.48 (m, 1H), 7.35–7.26 (m, 2H).

2-(4-methoxybenzylidene) malonic acid **20**: yield: 54%. ^{1}H NMR (400 MHz, DMSO) δ 7.78 (s, 1H), 7.50–7.46 (m, 1H), 7.46–7.41 (m, 1H), 7.14–7.07 (m, 1H), 7.01–6.96 (m, 1H).

Dimethyl 2-(cyclohexylmethylene) malonate **21**: yield: 88%. ^{1}H NMR (300 MHz, $CDCl_3$) δ 6.86 (d, J = 10.5 Hz, 1H), 3.84 (s, 3H), 3.78 (s, 3H), 2.39 (dd, J = 10.8, 3.3 Hz, 1H), 1.79–1.63 (m, 5H), 1.37–1.11 (m, 5H).

Dimethyl 2-(2-nitrobenzyl) malonate **22**: yield: 62%. ^{1}H NMR (300 MHz, $CDCl_3$) δ 8.04-8.01 (m, 1H), 7.58–7.53 (m, 1H), 7.47–7.37 (m, 2H), 3.94 (t, J = 7.6 Hz, 1H), 3.72 (s, 6H), 3.53 (d, J = 7.6 Hz, 2H).

(*E*)-Methyl 3-(2-nitrophenyl) acrylate **23**: ^{1}H NMR (300 MHz, $CDCl_3$) δ 8.14 (d, J = 15.8 Hz, 1H), 8.09–8.04 (m, 1H), 7.69–7.64 (m, 2H), 7.60–7.54 (m, 1H), 6.39 (d, J = 15.8 Hz, 1H), 3.85 (s, 3H).

3.2. Cell culture and inhibitor treatment

Each compound is dissolved at a concentration of 10 mM in DMSO. Murine macrophage RAW 264.7 (American Type Culture Collection, Rockville, MD) were routinely cultured at 37 °C in a humidified 5% CO_2 atmosphere in RPMI 1640 supplemented with 10% fetal bovine serum, penicillin (100 units/mL), and streptomycin sulfate (100 μg/mL). Cells placed in a 96-well plate at a density of 7.5×10^4 cells/well were incubated for 24 h. Cultured cells were treated with vehicle (control) and various concentrations of compound and then stimulated with 20 ng/mL of LPS for 24 h.

3.3. Cell viability assay

Cell viability was determined by (4-[3-(4-iodophenyl)-2-(4-nitrophenyl)-2*H*-5-tetrazolio]-1, 3-benzene disulfonate, WST-1) assay using Clontech premixed WST-1 cell proliferation reagent according to the manufacturer's instructions. Briefly, cells were inoculated at a density of 2×10^4 cells/well into 96-well plate and cultured at 37 °C for 24 h. The culture medium was replaced with 100 μL serum free medium and cultured cells were treated with vehicle (control) and various concentrations of compound. After 24 h, 10 μL premixed WST-1 solution was added to each well. After incubation at 37 °C for 30 min, the absorbance at 490 nm was measured using a microplate reader.

3.4. Measurement of NO

RAW 264.7 cells were placed in a 96-well plate at a density of 7.5×10^4 cells/well and incubated for 24 h. On the treatment day, media was removed and replaced with RPMI 1640 medium. Cultured cells were treated with vehicle or various concentration of compound then stimulated with 20 ng/mL LPS for 24 h. The nitrite concentration in the cultured media was measured as an indicator of NO secretion. Culture media (100 μL) were mixed with 10 μL of 2,3-diaminonaphthalene (0.05 mg/mL in 0.62 M aqueous HCl solution). After 15 min incubation in the dark, 5 μL of a 3 M aqueous NaOH solution was added to each well. Then, absorbance of the mixture at 450 nm was measured with a microplate reader.

3.5. Screening for NO production inhibitors

For screening of the 1364-compound NCI Diversity Set II library, the murine macrophage RAW 264.7 based nitric oxide (NO) assay was used. The library compounds (final concentration were 10 μM) were added in duplicate. Hits were qualified as compounds that reduced LPS-induced nitric oxide (NO) production by 90% or more at a concentration of 10 μM. The inhibition rate (%) of NO release was determined using the following formula: inhibition (%) = (OD450 value of LPS and vehicle treated group–OD450 value of compound treated group)/(OD450 value of LPS and vehicle treated group-OD450 value of vehicle treated group) × 100. For validation, positive and negative control wells were also included that consisted of LPS-activated cells without inhibitor and LPS-activated cells with TAK242.

To ascertain relative potencies of the most effective hits, we further assessed the activities of the compounds that showed more than 90% inhibition of the NO production at the initial concentration of 10 μM. Secondary screening was performed using the Nitric Oxide assay at a compound concentration of 1 μM in triplicate. Compounds exhibiting the inhibitory by 80% or more were subjected to a toxicity analysis.

3.6. TLR specificity test

This assay was performed using the same protocol with "3.4 Measurement of NO" as previously described. Instead of LPS, polyriboinosinic:polyribocytidylic acid (Poly(I:C)), FSL-1 ((S,R)-(2,3-bispalmitoyloxypropyl)-Cys-Gly-Asp-Pro-Lys-His-Pro-Lys-Ser-Phe), R848 (4-amino-2-(ethoxymethyl)-α, α-dimethyl-1*H*-imidazo[4,5-*c*]quinoline-1-ethanol) and Pam_3CSK_4 (*N*-palmitoyl-*S*-[2,3-bis(palmitoyloxy)-(2*RS*)-propyl]-[*R*]-cysteinyl-[*S*]-seryl-[*S*]-lysyl-[*S*]-lysyl-[*S*]-lysyl-[*S*]-lysine·3HCl) were used to selectively activate TLR3, TLR2/6, TLR7/8 and TLR1/2, respectively.

3.7. Dual luciferase report assay

NF-κB dual luciferase reporter BV-2 cells were cultured in DMEM medium supplemented with 10% FBS, penicillin (100 unit/mL), streptomycin (100 μg/mL) and puromycin (3 μg/mL). BV-2 reporter cells were seeded at a density of 1×10^4 cells/well in 96-well plates. After 24 h incubation, medium was changed to Opti-MEM medium supplemented with 0.5% FBS and indicated concentration of compound was added, and then stimulated with 200 ng/mL of LPS. After further 24 h treatment, the NF-κB activity was analyzed by Dual-Glo Luciferase Assay System. The ratio of Firefly luciferase activity to Renilla luciferase activity represents the NF-κB activity.

3.8. Measurement of cytokines

RAW 264.7 cells (5×10^5/well) pretreated with or without LPS, followed by treatment with indicated compound in 6-well plates. After 24 h, supernatants were harvested, clarified by centrifugation, and stored at −80 °C prior to analysis. Cells were collected and lysed by mammalian protein extraction reagent (Thermo Scientific, Rockford, IL, USA). Cell lysates were centrifuged at 1.3k rpm for 30 min at 4 °C, the supernatant were collected and stored at −80 °C prior to analysis. RAW 264.7 cell lysate IL-1β levels and RAW 264.7 cell media TNF-α levels were determined by enzyme-linked immunosorbent assay (ELISA) (BD Bioscience, San Diego, CA, USA) following the manufacturer's protocol. The total amount of the IL-1β was normalized to the total protein concentration.

3.9. Molecular modeling

Docking simulation of **1** was carried out using the Glide 5.6 program,[31,36] and the crystal structure of human TLR4–MD-2–LPS was cited from Protein Data Bank (3FXI).[5] The TLR4–MD-2–LPS complex orientations and conformations were prepared using standard Glide protocol and compound **1** was created with multiple conformational states and all possible rotational orientations.[37] **1** was final docked using standard Glide.

Acknowledgments

We thank the National Institutes of Health (DA026950, DA025740, NS067425, and DA029119) for financial support of this work. S.Z. thanks the support of China Scholarship Council (Grant No. 2009604039).

Supplementary data

Supplementary data associated with this article can be found, in the online version, at http://dx.doi.org/10.1016/j.bmc.2012.08.022.

References and notes

1. Akira, S.; Uematsu, S.; Takeuchi, O. *Cell* **2006**, *124*, 783.
2. Akira, S. *Curr. Top. Microbiol. Immunol.* **2006**, *311*, 1.
3. Dauphinee, S. M.; Karsan, A. *Lab Invest.* **2006**, *86*, 9.
4. Raetz, C. R.; Whitfield, C. *Annu. Rev. Biochem.* **2002**, *71*, 635.
5. Park, B. S.; Song, D. H.; Kim, H. M.; Choi, S.; Lee, H.; Lee, J. *Nature* **2008**, *458*, 1191.
6. Saitoh, S.; Akashi, S.; Yamada, T.; Tanimura, N.; Kobayashi, M.; Konno, K.; Matsumoto, F.; Fukase, K.; Kusumoto, S.; Nagai, Y.; Kusumoto, Y.; Kosugi, A.; Miyake, K. *Int. Immunol.* **2004**, *16*, 961.
7. Collins, T.; Read, M. A.; Neish, A. S.; Whitley, M. Z.; Thanos, D.; Maniatis, T. *FASEB* **1995**, *9*, 899.
8. Zhang, G.; Ghosh, S. *J. Clin. Invest.* **2001**, *107*, 13.
9. Karin, M.; Ben-Neriah, Y. *Annu. Rev. Immunol.* **2000**, *18*, 621.
10. Hawiger, J. *Immunol. Res.* **2001**, *23*, 99.
11. Tian, B.; Brasier, A. R. *Recent Prog. Horm. Res.* **2003**, *58*, 95.
12. Hennessey, E. J.; Parker, A. E.; O'Neill, L. A. *Nat. Rev. Drug Disc.* **2010**, *9*, 293.
13. Guo, L. H.; Schluesener, H. J. *Cell. Mol. Life Sci.* **2007**, *64*, 1128.
14. Friedman, W. J. *Exp. Neurol.* **2001**, *168*, 23.
15. Sian-Marie Lucas, S.; Rothwell, N. J.; Gibson, R. M. *Br. J. Pharmacol.* **2006**, *147*, S232.
16. Carcillo, J. A. *Crit. Care Clin.* **2003**, *19*, 413.
17. Serhan, C. N.; Savill, J. *Nat. Immunol.* **2005**, *6*, 1191.
18. Rocha, V. Z.; Libby, P. *Nat. Rev. Cardiol.* **2009**, *6*, 399.
19. Rakoff-Nahoum, S. *Yale J. Biol. Med.* **2006**, *79*, 123.
20. Buchanan, M. M.; Hutchinson, M. R.; Watkins, L. R.; Yin, H. *J. Neurochem.* **2010**, *114*, 13.
21. Ii, M.; Matsunaga, N.; Hazeki, K.; Nakamura, K.; Takashima, K.; Seya, T.; Hazeki, O.; Kitazaki, T.; Iizawa, Y. *Mol. Pharmacol.* **2006**, *69*, 1288.
22. Mullarkey, M.; Rose, J. R.; Bristol, J.; Kawata, T.; Kimura, A.; Kobayashi, S.; Przetak, M.; Chow, J.; Gusovsky, F.; Christ, W. J.; Rossignol, D. P. *J. Pharmacol. Exp. Ther.* **2003**, *304*, 1093.
23. Rice, T. W.; Wheeler, A. P.; Bernard, G. R.; Vincent, J. L.; Angus, D. C.; Aikawa, N.; Demeyer, I.; Sainati, S.; Amlot, N.; Cao, C.; Ii, M.; Matsuda, H.; Mouri, K.; Cohen, J. *Crit. Care Med.* **2010**, *38*, 1685.
24. Bloomberg web site. http://www.bloomberg.com/news/2011-01-25/eisai-s-sepsis-drug-eritoran-fails-to-save-more-lives-in-final-stage-study.html. Posted 25.01.11.
25. Nussler, A. K.; Glanemann, M.; Schirmeier, A.; Liu, L.; Nüssler, N. C. *Nat. Protoc.* **2006**, *1*, 2223.
26. Ngamwongsatit, P.; Banada, P. P.; Panbangred, W.; Bhunia, A. K. *J. Microbiol. Methods* **2008**, *73*, 211.
27. Mullarkey, M.; Rose, J. R.; Bristol, J.; Kawata, T.; Kimura, A.; Kobayashi, S.; Przetak, M.; Chow, J.; Gusovsky, F.; Christ, W. J.; Rossignol, D. P. *J. Pharmacol. Exp. Ther.* **2003**, *304*, 1093.
28. Takashima, K.; Matsunaga, N.; Yoshimatsu, M.; Hazeki, K.; Kaisho, T.; Uekata, M.; Hazeki, O.; Akira, S.; Iizawa, Y.; Ii, M. *Br. J. Pharmacol.* **2009**, *157*, 1250.
29. Guterman, L. *Chem. Eng. News* **2011**, *89*, 19.
30. Liu, S.; Kielian, T. *J. Immunol.* **2009**, *183*, 5537.
31. Cheng, K.; Wang, X.; Yin, H. *J. Am. Chem. Soc.* **2011**, *133*, 3764.
32. Bevan, D. E.; Martinko, A. J.; Loram, L. C.; Stahl, J. A.; Taylor, F. R.; Joshee, S.; Watkins, L. R.; Yin, H. *ACS Med. Chem. Lett.* **2010**, *1*, 194.
33. Dziarski, R.; Gupta, D. *J. Endotoxin Res.* **2000**, *6*, 401.
34. Adediran, S. A.; Cabare, D.; Lohier, J.-F.; Wakselman, M.; Pratt, R. F. *Bioorg. Med. Chem.* **2010**, *18*, 282.
35. Chang, S.; Yin, S.-L.; Wang, J.; Jing, Y.-K.; Dong, J.-H. *Molecules* **2009**, *14*, 4166.
36. Glide, version 5.6; Schrödinger, LLC: New York, NY, 2010.
37. Halgren, T. A.; Murphy, R. B.; Friesner, R. A.; Beard, H. S.; Frye, L. L.; Pollard, W. T.; Banks, J. L. *J. Med. Chem.* **2004**, *47*, 1750.